

**The Study of the C_{60}^+ Cation in a Supersonic Slit Jet
Using Cavity Ring Down Spectroscopy**

Christopher P. Morong

October 24, 2003
2:30-4:00 PM Kent 102

Candidacy Committee: Butler, Sibener, Norris

Critical Review: S. Rudić, et al., PCCP 5 (2003) 1205-1212

Introduction:

Since buckminsterfullerene (C_{60}) was discovered in 1985 by Kroto, Smalley and Curl,¹ it has been a molecule of considerable interest both for its potential applications on Earth and as a possible carrier for some of the diffuse interstellar bands (DIBs) in the near infrared.² The DIBs are comprised of over 600 unidentified spectroscopic absorption features which are too broad to be atomic lines and are only seen in interstellar space. Laboratory identification of these features has thus far remained elusive, but several candidate classes of molecules have been suggested as carriers, including polycyclic aromatic hydrocarbons (PAHs), carbon chains, fullerenes, solid particles and simple molecules in either the neutral or ionized states.³ Certain DIBs have a strong intensity correlation between sources and are known as families. Two DIBs at 9577 Å and 9632 Å have a correlation of greater than 0.9 indicating a common molecular carrier and form one such family.⁴ These have been tentatively identified as due to C_{60}^+ due to

resemblances between the DIB spectra and the spectra measured in solid matrices of argon and neon² (Figure 1).

Under the assumption that these two DIBs are C_{60}^+ , it has been estimated that between 0.26% and 1.7% of interstellar carbon is in the form of C_{60}^+ . This is significant in comparison to the estimated ~10-15% in interstellar carbon in the form of PAHs and will have an effect on interstellar chemistry.^{5,6} Once gas phase measurements are performed, the tentative assignment can be confirmed or denied.

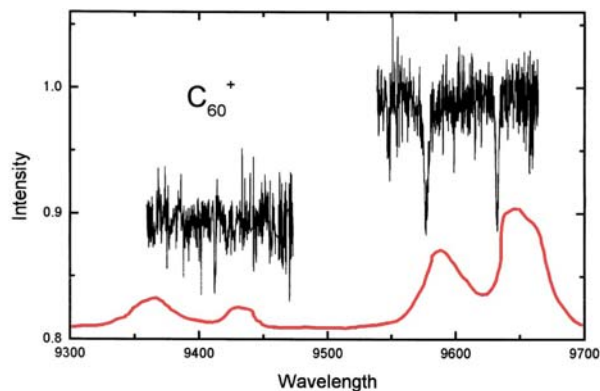


Figure 1 – The experimentally observed spectrum of C_{60}^+ in a solid neon matrix (red) compared to the observed DIBs (black).¹⁹ The intensity differences, broadening and peak shifts can be due to perturbations from the solid matrix. The vibronic lines around 9400 Å are not seen in the DIBs perhaps due to the lower intensity.

I propose to study the electronic spectrum of C_{60}^+ by cavity ring down spectroscopy (CRDS) in a supersonic slit jet using a continuous wave Ti:Sapphire laser. The slit jet has been assembled and operated for short periods but not experimentally used.⁷ The Ti:Sapphire laser has been used extensively for H_3^+ ⁸ and solid hydrogen work⁹ but has not been used in the long wave optics region around 9600 Å and needs to be fiber optically coupled to the slit jet because the devices are in different rooms. Cavity ring down is a completely

new method of multipassing for the Oka group and is capable of reaching new levels of sensitivity in the slit jet to record weak absorbances.

Electronic Structure

C_{60} is a truncated icosahedron composed of 12 pentagons and 20 hexagons in the I_h group.¹⁰ Upon ionization, the Jahn-Teller effect reduces the symmetry to D_{5d} or D_{3d} .^{11,12} Ab initio computational studies have indicated that the Jahn-Teller stabilization energy of the six equivalent D_{5d} structures is 0.35 eV lower compared to the optimized I_h structure. The ten equivalent D_{3d} structures only have a stabilization energy 0.10 eV lower compared to the optimized I_h structure. The D_{5d} structure has a ${}^2A_{1u}$ electronic ground state and is the true equilibrium structure. The six equivalent D_{5d} structures can interconvert by a pseudo-rotation pathway involving a ${}^2B_{1u}$ transition state with D_{2h} symmetry that has a barrier height of 0.09 eV.¹³

C_{60} has a low ionization energy of 7.61 eV, which is between that of iron (7.87 eV) and titanium (6.82 eV). The second ionization potential of iron and titanium is 16.18 eV and 13.58 eV respectively, while for C_{60} it is 19 eV. In diffuse clouds both iron and titanium have greater abundance as singly charged cations than neutrals or doubly charged cations, implying that if interstellar C_{60} exists, it will exist as a singly charged cation.¹⁴ The strength of the C_{60}^+ DIBs are highest in areas with a high abundance of UV radiation - diffuse clouds with a density on the order of 10^2 molecules/cm³. The abundance decreases in dense clouds where UV radiation has less penetration power.¹⁵

Spectroscopy

Electronic spectroscopy of C_{60}^+ has only been done in solid matrices of Freon,¹⁶ argon¹⁷ and neon.¹⁸ Intermediate neglect of differential overlap (INDO) calculations done by Bendale indicate that the 0_0^0 transition of the ${}^2E_{1g} - {}^2A_{1u}$ band occurs at 8630 cm⁻¹ or 11587 Å. A single broad peak at 10200 cm⁻¹ was first observed in a glassy Freon matrix.¹⁶ Later matrix experiments have resolved two absorption peaks at 10282 cm⁻¹ and 10355 cm⁻¹ in an argon matrix¹⁷ and at 10368 cm⁻¹ and 10435 cm⁻¹ in a neon matrix.¹⁸ The two DIBs have been observed at 9632 Å and 9577 Å (10382 cm⁻¹ and 10442 cm⁻¹, respectively). The cause of

the 60 cm^{-1} splitting is not completely known, but is thought to be due to the static Jahn-Teller effect. It is not believed to be a vibronic transition because the energy is too low.¹⁹ The nearest experimentally observed vibronic peaks exist between 9350-9450 Å (Figure 1).

From the spectra obtained, the possible identification of the DIBs at 9577Å and 9632Å as due to C_{60}^+ has been suggested, but not universally accepted.¹⁵ The solid matrices cause significant shifts on the order of 100 cm^{-1} , however these values are estimates based on matrix and gas phase measurements of simpler molecules. The tentative identification has not been universally accepted because the gas phase measurements have not been performed successfully, because the vibronic and visible absorptions of the neutral C_{60} have not been observed in the DIBs, and because of a difference between intensity ratios of the astronomical and laboratory doublet spectra. A possible vibronic band may have been seen in the DIBs at 9410 Å but is not definitive because of the weaker intensities and significant telluric interferences.⁴ Neutral C_{60} would be depleted from constant irradiation to produce the cation. Relative intensity differences could be due to perturbations caused by the solid matrix.

Carbon-12 is a boson with a nuclear spin of zero, which significantly affects the allowed rotational levels. To a first approximation the total wave function Ψ of the molecule can be factored into electronic (Ψ_{el}), vibrational (Ψ_{vib}), rotational (Ψ_{rot}), and nuclear spin (Ψ_{ns}) parts.

$$\Psi = \Psi_{el} \Psi_{vib} \Psi_{rot} \Psi_{ns} \quad (1)$$

Since the carbon is a boson, Ψ has to be in either the symmetric A_{1g} or A_{1u} representations because the inversion operation cannot occur without breaking bonds. Ψ_{ns} has to be in the totally symmetric A_{1g} representation.^{20,21} The ground vibrational state is in the totally symmetric A_{1g} representation. The electronic ground and excited states have A_{1u} and E_{1g} symmetry, respectively. Therefore the allowed ground rotational wavefunction must contain A_{1u} or A_{1g} and the excited rotational wavefunction must contain E_{1g} or E_{1u} . From Weber,²² the allowed ro-vibronic ground states are for $J=\text{even}, K=0$ and $J=\text{all}, K=5p$ and $J \geq K$ where p is a positive non-zero integer. The allowed excited ro-vibronic states are for $J=\text{all}, K=5p \pm 1$. Finally the allowed transitions are $\Delta J = 0, \pm 1$ and $\Delta K = \pm 1$.

The following values were obtained from the INDO calculations¹³ to determine the geometric shape of C_{60}^+ and the order of magnitude perturbations due to the Jahn-Teller effect and isotopic substitution. Depending on the geometry, the number of symmetry unique carbons and bond types changes. For an I_h geometry there is one unique carbon and two unique bond types. For D_{5d} symmetry there are four unique carbons with seven unique bond types. For D_{2h} symmetry there are nine unique carbons with fifteen unique bond types.²³ The moment of inertia splits from 6040 amu \AA^2 for spherical C_{60} to a prolate symmetric top with $I_A = 5999$ amu \AA^2 and $I_B = I_C = 6073$ amu \AA^2 yielding rotational constants of $A = 2.810 \times 10^{-3} \text{ cm}^{-1} = 84.24 \text{ MHz}$ and $B = C = 2.776 \times 10^{-3} \text{ cm}^{-1} = 83.22 \text{ MHz}$. The rotational energy of a prolate symmetric top is given by

$$E_{JK} = BJ(J+1) + (A-B)K^2 \quad (2)$$

Using the spin statistics, the spacing between the J rotational lines will be on the order of 300 MHz and the K rotational lines around the J level will be on the order of 10 MHz.

A natural ‘‘contaminant’’ in the C_{60} system that can reduce the symmetry further is ^{13}C which has a 1.1% abundance. Only 51% will exist as $^{12}\text{C}_{60}^+$, 34% will exist as $^{13}\text{C}^{12}\text{C}_{59}^+$, 11% will exist as $^{13}\text{C}_2^{12}\text{C}_{58}^+$ and 4% will have more than two ^{13}C atoms. The effect of one ^{13}C is to reduce the symmetry further to C_s .²⁰ Although numerically the effect is less than the change caused by the Jahn-Teller distortion. The fermion lifts the strict boson-exchange exclusion for pure $^{12}\text{C}_{60}^+$, permitting all the rotational lines to exist with a spacing of approximately 150 MHz. It is also important to consider that the Doppler broadening at 10 K is about 30 MHz. The instrumental resolution is limited by the laser bandwidth of approximately 500 kHz. It appears that $^{12}\text{C}_{60}^+$ can be rotationally resolved.

Supersonic Slit Jet

A supersonic expansion occurs when a high pressure source is allowed to adiabatically expand into a low pressure chamber (Figure 2). The gas has a high velocity perpendicular to the slit, but a low velocity parallel to the slit. The random thermal motion of the high pressure gas is converted to directed motion, narrowing the velocity distribution and shifting it to a nonzero value.²⁴ Therefore in the reference frame of the

gas, it is very cold, with rotation and translation temperatures on the order of 10 K. The translation-rotation-vibration relaxation process occurs from collisions at different rates. For the short time the molecules are in the discharge, the cooling among the different degrees of freedom is not equivalent. The energy transfer between translational degrees of freedom occurs on the order of 10^{-9} s. The energy transfer between rotation and translation is on the order of 10^{-8} s, and between vibration and translation the

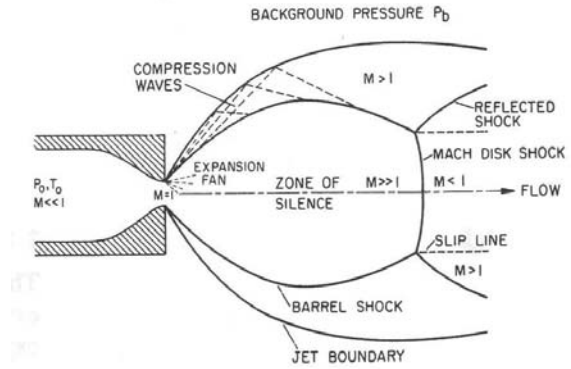


Figure 2 – The structure of the supersonic expansion. The gas flows with a high velocity along the flow vector, but with a low velocity perpendicular to the flow. The area that will be probed is the zone of silence where the gas moves with a speed greater than the local speed of sound because it consists of cold molecules in a collisionless environment. The centerline Mach number falls along the dotted flow line.²⁶

energy transfer is on the order of 10^{-5} s, which is comparable to the transit time through the slit. The vibrational cooling is not as drastic as the rotational and translational cooling and may cause the appearance of hot vibrational bands at different intensities than a true equilibrium mixture.²⁵

The pressure, P , temperature, T , and density, ρ , in the expansion are completely described by the initial conditions of the high pressure gas (P_0, T_0 and ρ_0), the ratio of specific heats, γ , and the Mach number, M .

$$\frac{T}{T_0} = \left(\frac{P}{P_0}\right)^{(\gamma-1)/\gamma} = \left(\frac{\rho}{\rho_0}\right)^{(\gamma-1)} = \left(1 + \frac{\gamma-1}{2} M^2\right)^{-1} \quad (3)$$

The Mach number is the ratio of the speed of the particle to the local speed of sound and is determined from an expansion in terms of the ratio between the distance from the slit, x , and the slit width, d , and the ratio of specific heats. A complete table of values and formulas for a slit or circular orifice can be found in Scoles.²⁶ Technically the values used for slits are derived for infinitely long slits, but in general the solutions are valid as long as the length is much greater than the width.

The Mach number does not increase indefinitely. As seen in Figure 2, the shockwaves on the outside of the expansion eventually cause the formation of a Mach disk that abruptly terminates the expansion, raising the temperature, pressure and density as the gas becomes subsonic. The location of the Mach disk, x_M , is insensitive to the type of gas and depends on the background chamber pressure P_b , stagnation pressure and slit

width and is given by $x_M \approx 0.67d\sqrt{(P_0/P_b)}$. Under optimal conditions we should be able to produce a Mach disk up to 1 cm from the slit.

Cavity Ring Down Spectroscopy:

Cavity ring down spectroscopy (CRDS) allows for kilometer long pathlengths in a cell, making it possible to observe extremely small absorbences on the order of 10^{-11} /cm. A laser beam enters a high finesse cavity composed of two highly reflective confocal dielectric mirrors with reflectivities greater than 99.99% separated by less than twice their radius of curvature. Only a small fraction enters the cavity because of back reflections, but the intensity, I , exiting the second mirror decays exponentially as

$$I(t) = I_0 e^{-t/\tau(\nu)} \tag{4}$$

and is recorded as the intensity in the cavity decreases as the light leaks out. The time constant, $\tau(\nu)$, on the order of 30 μ s contains the absorbance information by

$$\tau(\nu) = \frac{d}{c(1 - R(\nu) + NL\sigma(\nu))} \tag{5}$$

where c is the speed of light, d is the distance between the mirrors, $R(\nu)$ is the reflectance dependence on the frequency, N is the number density, L is the length of the sample, and $\sigma(\nu)$ is the cross sectional dependence on the frequency. The time constant for the empty cavity can easily be found by setting the number density to zero.²⁷

Initially pulsed lasers were used, but recently with the addition of an acousto optic modulator (AOM) which

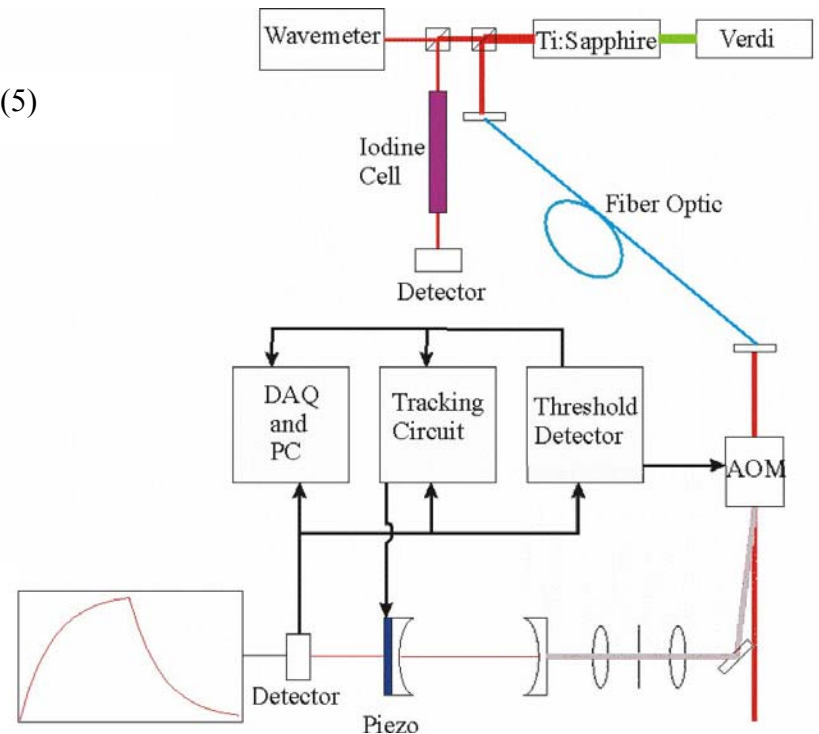


Figure 3 – The cavity ring down experimental apparatus. A 10 W Verdi (green) pumps a Ti:Sapphire crystal to lase in the near infrared. The wavelength is measured using a wavemeter and an iodine reference. Fiber optics bring the beam to the acousto optic modulator (AOM) which deflects the laser into the cavity to increase the intensity (gray) or allows the laser to pass (red) allowing the light to decay and the ring down signal to be recorded. The tracking circuit uses the piezo to mode match the cavity to the laser and the threshold detector controls measures the intensity and controls the AOM.

deflects the beam off the cavity effectively chopping the laser, continuous wave lasers can be used (Figure 3). The laser is mode matched to the TEM₀₀ modes of the cavity using the two lenses and a pinhole before the cavity. A piezo is used to modulate the cavity length to make the frequency of one of the cavity modes oscillate around the laser line. The laser pumps up the cavity until a photodiode registers enough intensity to trigger the AOM and deflects the laser beam allowing the ring down signal to be recorded.^{28,29} This can be considered an optical analog of an RC circuit.

Experimental

A former graduate student in the Oka group, Mike Lindsay, designed and assembled the supersonic slit jet apparatus⁷ to be used with a Herriot cell by placing two spherical mirrors at slightly less than twice their radius of curvature which allows for about 20 passes through a 4 cm path length. Unlike other designs that use a pulsed jet,^{30,31,32,33,34} our design uses a continuous source, allowing for faster scans. After initial testing, it was discovered that the slit materials degraded in the plasma. I changed the materials from steel to lower sputtering aluminum for the slits and from Macor to alumina for the insulator. The new materials are much more stable in an air plasma. I have redesigned and built the high pressure source to allow for easy vertical movement to scan different areas in the expansion without realigning all the optics. A water cooling line was added to maintain a more stable temperature in the stagnation gas while the plasma is ignited. This could easily be adapted for liquid nitrogen cooling. A negative potential is applied to the exit slit while the entrance slit remains grounded, causing the electrons to travel antiparallel to the gas flow producing more electron particle collisions. A square wave voltage chopper can also be used to concentration modulate the plasma, in order to obtain a better S/N. Ballast resistors with an equivalent resistance of 1250 Ω are used to prevent excessive currents that could damage the electronics. The slit allows for more of the gas to expand down rather than outwards resulting in much narrower line widths.

Although C₆₀ is a solid at room temperature, there is a small vapor pressure that is increased through heating. Piacente experimentally determined the vapor pressure at high temperatures to be³⁵

$$\log\left(\frac{P}{\text{kPa}}\right) = (8.28 \pm 0.20) - \frac{(9154 \pm 150)}{T(\text{K})} \quad (6)$$

Several groups^{18,20} have used temperatures around 800 K for gas phase studies, corresponding to pressures of 10 millitorr. Higher temperatures could be used if the helium is used as the carrier gas for C₆₀. It is difficult to determine the amount of C₆₀ that will condense out as it travels to the aperture from cooling. A possible complication is that supersonic expansions, while making the ions rotationally cool, do not always vibrationally cool the molecules considerably. There may be a discrepancy between the intensities of the vibrational bands between laboratory and interstellar measurements.

To determine if C₆₀⁺ can be observed in the slit jet, known experimental absorbances must be compared with the theory. The width ($\Delta\nu$) of the DIB lines is 3.1 cm⁻¹. Lower bounds on the oscillator strength (f) for C₆₀⁺ are 0.003-0.006,¹⁹ which is related to the extinction coefficient (ϵ) by

$$f = \frac{4\epsilon_0 m_e c^2 (\ln 10)}{N_A e^2} \int_{\nu_1}^{\nu_2} \epsilon(\nu) d\nu \approx 4.319 \times 10^{-10} \left(\frac{\text{mol}}{\text{m}} \right) \epsilon_{\text{max}} \Delta\nu \quad (7)$$

yielding a lower bound on the peak of the extinction coefficient of $2 \times 10^4 \text{ m}^2 \text{ mol}^{-1}$.

Fulara performed matrix spectroscopy on the cation by mass selecting the C₆₀⁺ and codepositing it with neon. From the ion currents and deposition time a density of 10^{16} ions/cm³ was estimated for a total path length of 1 cm.³⁶ The experimental absorbances were not given, but from the oscillator strength and peak width, an estimated maximum absorbance of 0.4 is found. With CRDS having sensitivities approaching 10^{-11} /cm, it should be possible to make and detect concentrations of a few hundred thousand ions per cm³.

Complications

In the spectral range of the DIBs, a major contaminant is atmospheric water that causes many telluric interference lines. Fortunately these lines are well documented for astronomical and environmental applications and can serve as a reference gas. However, the water absorbances can lead to losses in the Ti:Sapphire laser cavity making it difficult to lase. The laser needs to be placed in a box that is purged with dry nitrogen to obtain the best results.

Velocity modulation of the plasma at kHz frequencies is a technique that has been used extensively in the Oka group for ion/neutral discrimination as well as mass selectivity and cation/anion discrimination. Unfortunately velocity modulation techniques have not yet been successful in slit jet discharges. Difficulties

include arcing as the plasma is drawn to the electrodes and Debye shielding that prevents an electric field from existing in the plasma.³⁰ We will not be able to determine if the absorbance is due to an ion or a neutral.

Frequency modulation of the laser at MHz frequencies is a more recent technique that has been used in the Oka group to reduce laser noise. It has been coupled to CRDS but instead of using a continuously modulated laser as the Oka group does, the ring down signal for two different frequencies that are temporally out of phase is measured.³⁷ The advantage to coupling it to CRDS is the ability to measure the cavity properties at absorption and non-absorption points in a short time interval, allowing the properties of the cavity to be measured and reducing noise from fluctuations in the plasma. Once the CRDS is successfully implemented, this is an avenue worth examining.

Conclusions

The identification of the DIBs at 9577 Å and 9632 Å has important implications for interstellar chemistry. Currently it is believed that upwards of 1.7% of interstellar carbon is in the form of C_{60}^+ and is responsible for these peaks. Determining the exact location of the spectral bands is an important step toward identifying the DIBs and understanding the interstellar chemistry. Due to large matrix effects which may have shifted the C_{60}^+ bands by over 100 cm^{-1} , the search for the gas phase values may prove difficult. Fortunately the location of the two DIB peaks are known to great accuracy from the astronomical observations and this is the location to examine first. If nothing is seen it could mean either the sensitivity is not high enough, the ion concentration is not high enough, or the DIB peaks are not due to C_{60}^+ . The first two can be checked experimentally. If the observed DIB peaks are not due to C_{60}^+ , we will search of the surrounding spectral region. This could be time consuming, but doable in a realistic time.

References

-
- ¹ H.W. Kroto, *Angewandte Chemie*, **31** (1992) 111-129
 - ² B.H. Foing and P. Ehrenfreund, *Nature* **369** (1994) 296-298
 - ³ G.H. Herbig, *Annu. Rev. Astrophys.* **33** (1995) 19-73
 - ⁴ G. A. Galazutdinov, et al., *Mon. Not. R. Astron. Soc.* **317** (2000) 750-758
 - ⁵ P. Ehrenfreund and B.H. Foing, *Adv. Space Res.*, **19** (1997) 1033-1042
 - ⁶ C. Moutou, et. al., *Astron. Astrophys.*, **347** (1999) 949-956
 - ⁷ C.M. Lindsay *Research Prospectus*, University of Chicago, 1997
 - ⁸ J.L. Gottfried, B. McCall and T. Oka, *J. Chem. Phys.* **118** (2003) 10890-10899

-
- ⁹ R. Dickson, *Doctoral Thesis*, University of Chicago, 1996
- ¹⁰ A. Chang, W.C. Ermler and R.M. Pitzer, *J. Phys. Chem.* **95** (1991) 9288-9291
- ¹¹ C P Moate, J L Dunn, C A Bates and Y M Liu, *J. Phys.: Condens. Matter*, **9** (1997) 6049-6060
- ¹² A. Ceulemans and P.W. Fowler, *J. Chem. Phys.*, **93** (1990) 1221-1234
- ¹³ R.D. Bendale, J.F. Stanton and M.C. Zerner, *Chem. Phys. Lett.*, **194** (1992) 467-471
- ¹⁴ G.H. Herbig, *Astrophysical Journal*, **542** (2000) 334-343
- ¹⁵ P. Jenniskens, G. Mulas, I. Porceddu, and P. Benvenuti, *Astron. Astrophys.* **327** (1997) 337-341
- ¹⁶ T. Kato et al., *Chem. Phys. Lett.*, **180** (1991) 446-450
- ¹⁷ Z. Gasyna, L. Andrews, and P.N. Schatz, *J. Phys. Chem.*, **96** (1992) 1525-1527
- ¹⁸ J. Fulara, M. Jakobi and J.P. Maier, *Chem. Phys. Lett.*, **211** (1993) 227-234
- ¹⁹ J. Fulara and J.Krelowski, *New Astronomy Reviews* **44** (2000) 581-597
- ²⁰ N. Sogoshi et al., *J. Phys. Chem A*, **104** (2000) 3733-3742
- ²¹ R. Saito, G. Dresselhaus and M.S. Dresselhaus, *Phys. Rev. B*, **50** (1994) 5680-5688
- ²² A. Weber, *J. Chem. Phys.*, **73** (1980) 3952-3972
- ²³ N. Koga and K. Morokuma, *Chem. Phys. Lett.*, **196** (1992) 191-196
- ²⁴ D.H. Levy, *Science*, **214** (1981) 263-269.
- ²⁵ W. H. Flygare, *Acc. Chem. Rev.* **1** (1968) 121-127.
- ²⁶ G. Scoles, *Atomic and Molecular Beam Methods* Vol. 1, 14-53 Oxford (1988)
- ²⁷ T. G. Spence, et al., *Rev. Sci. Inst.*, **71** (2000) 347-353.
- ²⁸ D. Romanini, A.A. Kachanov, F. Stoeckel, *Chem. Phys. Lett.*, **270** (1997) 538-545
- ²⁹ D. Romanini, A.A. Kachanov, N. Sadeghi, E Stoeckel, *Chem. Phys. Lett.*, **264** (1997) 316-322
- ³⁰ S. Davis, *Doctoral Thesis*, University of Colorado, 1999.
- ³¹ M. Farnik, et al., *J. Chem. Phys.*, **116** (2002) 6146-6158
- ³² M. Hippler and M. Quack, *J. Chem. Phys.*, **116** (2002) 6045-6055
- ³³ T. Haber, U. Schmitt, and M.A. Suhm, *Phys. Chem. Chem. Phys.*, **1** (1999) 5573-5582
- ³⁴ M. Ishiguro, et al., *Chem. Phys. Lett.*, **263** (1996) 629-634
- ³⁵ V. Piacente, G. Gigli, P. Scardala, A. Giustini and D. Ferro, *J. Phys. Chem.* **99** (1995) 14052-14057
- ³⁶ J. Maier, Private correspondence
- ³⁷ J. Ye and J.L. Hall, *Phys. Rev. A*, **61** (2000) 061802